Bio-Design and Manufacturing (2022) 5:348–357
https://doi.org/10.1007/s42242-021-00155-2

RESEARCH ARTICLE

# Coaxial bioprinted microfibers with mesenchymal stem cells for glioma microenvironment simulation

Zhizhong Jin[1] · Xinda Li[2] · Boxun Liu[3] · Xinru Yan[4] · Shuai Han[1] · Tao Xu[2,3] · Anhua Wu[1]

Received: 12 November 2020 / Accepted: 19 June 2021 / Published online: 25 September 2021
© Zhejiang University Press 2021

## Abstract

Due to their special anatomical and physiological features, central nervous system diseases still presented challenges, despite the fact that some advances have been made in early diagnosis and precision medicine. One of the complexities in treating tumors is the tumor microenvironment, which includes mesenchymal stem cells (MSCs) that exhibit tumor tropism and can be used for cell therapy. However, whether MSCs promote or suppress gliomas is still unclear, especially in glioma microenvironments. In this study, a coaxial microfiber was designed to mimic the tumor microenvironment and to reveal the effect of MSCs on glioma cells. The fiber shell was composed of MSCs and alginate, and the core was filled with U87MG (glioblastoma) cells and gelatin methacrylate. This Shell-MSC/Core-U87MG microenvironment improved the proliferation, survival, invasion, metastasis, and drug resistance of glioma cells, while simultaneously maintaining the stemness of glioma cells. In summary, coaxial extrusion bioprinted Shell-MSC/Core-U87MG microfiber is an ideal platform for tumor and stromal cell coculture to observe tumor biological behavior in vitro.

## Graphic abstract

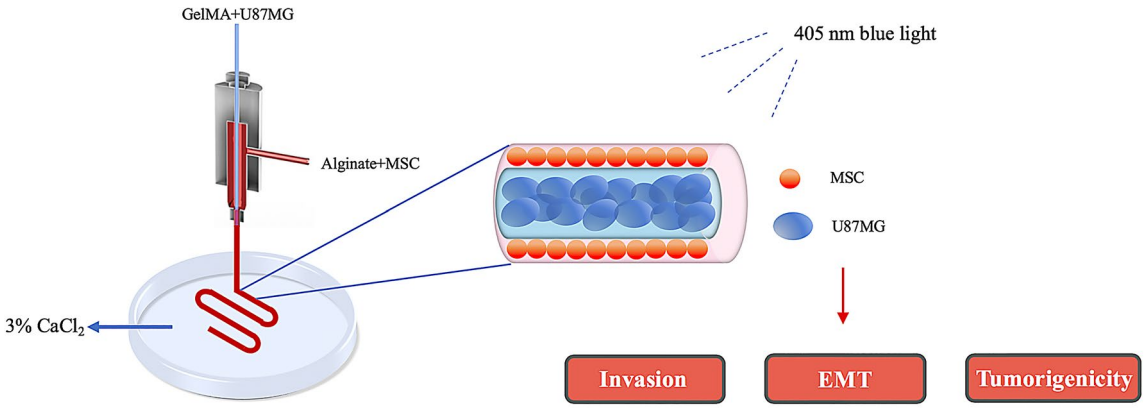


**Keywords** Coaxial bioprinting · GBM microenvironment · MSC · Coculture

✉ Tao Xu
taoxu@mail.tsinghua.edu.cn

✉ Anhua Wu
ahwu@cmu.edu.cn

[1] Department of Neurosurgery, The First Hospital of China Medical University, Shenyang 110001, China

[2] Biomanufacturing and Rapid Forming Technology Key Laboratory of Beijing, Department of Mechanical Engineering, Tsinghua University, Beijing 100084, China

[3] Department of Precision Medicine and Healthcare, Tsinghua-Berkeley Shenzhen Institute, Shenzhen 518055, China

[4] East China Institute of Digital Medical Engineering, Shangrao 334000, China

## Introduction

Glioblastoma (GBM) is the most common and fatal type of primary central nervous system (CNS) tumor [1]. The current treatment is surgical resection followed by postoperative radiotherapy and adjuvant chemotherapy. However, the treatment has unsatisfactory results, with median survival rates of 12–15 months after the resection surgery [2]. With increased understanding of the biological features of gliomas, scientists have realized that the glioma microenvironment affects the occurrence and progression of gliomas. In addition to inflammatory cells, tumor-associated fibroblasts and stromal cells, as well as mesenchymal stem cells (MSCs), are actively attracted to primary tumor sites [3, 4]. In the past, many MSCs were used as carriers to reach tumor targets for cell therapy because of tumor tropism and achieved initial results [5, 6].

However, whether MSCs themselves affect gliomas is a continuing focus in the scientific community. Both pro- and anti-tumorigenic effects have been reported [7–9]. Since these cells have a two-way effect in vitro, the key to the problem lies in the effect of MSCs on glioma cells in the tumor microenvironment. Accordingly, we chose the coaxial bioprinting method to manufacture a tumor microenvironment to facilitate observation of the effect of MSCs on U87MG glioma cells. This coaxial microenvironment was composed of a shell portion and a core portion; the shell was MSC-alginate, and the core was U87MG-GelMA. Such a Shell-MSC/Core-U87MG microenvironment provides a 3D structure and an extracellular matrix (ECM) similar to those found in vivo, which ensures that the spatial cell arrangement and the cell behavior in ECMs can be distinguished from two-dimensional (2D) planar culture [10]. At the current time, glioma models constructed with bioprinting platforms containing glioma cells or glioma stem cells have been reported, but there is no bioprinted glioma model with MSCs [11]. A glioma model with MSCs and ECMs is beneficial for mimicking the glioma microenvironment and studying the biological characteristics of glioma cells.

In this study, we fabricated Shell-MSC/Core-U87MG hydrogel microfibers to observe the effect of MSCs on glioma cells. In this microenvironment, we tested the morphology, proliferation, survival, and drug resistance of the U87MG cells in the core. In addition, we measured stemness and angiogenic ability, which determine the malignancy and tumorigenic ability of tumor cells. Finally, we explored the mechanism of increased spreading and invasion ability of U87MG cells derived from Shell-MSC/Core-U87MG microfibers, which may be related to enhancements imparted by MSCs to epithelial–mesenchymal transition (EMT) and matrix metalloproteinase 2 (MMP2) secretion ability.

## Materials and methods

### Cell culture

U87MG cells, adipose-derived MSCs (ADMSCs), and bone marrow-derived MSCs (BMMSCs) were purchased from ScienCell Research Laboratories (Sciencell, CA, USA) and cultured in Dulbecco's modified Eagle's medium supplemented with 10% fetal bovine serum (FBS), 1% (0.01 g/mL) L-glutamine, and 1% (0.01 g/mL) penicillin/streptomycin. After massive expansion, cells were used in bioprinting and culturing. The number of MSC generations did not exceed six.

### Coaxial bioprinting process

Before printing, U87MG cells were digested by TrypLE (ThermoFisher Scientific, Waltham, MA, USA) and MSCs were digested by Accutase (Stemcell Technologies, Vancouver, Canada). We printed the Shell–core hydrogel microfibers using a previously reported method with a custom-made extrusion bioprinting device [12]. The device had a sheath/core coaxial nozzle which allowed installation and disassembly. The inner and outer diameters of the print head were 21G and 16G, respectively. Alginate (0.01 g/mL; Sigma-Aldrich, Shanghai, China) solution with or without MSCs was used for the shell stream, and the extrusion rate was 15 mL/h; the core stream was composed of 5% GelMA (EFL, Suzhou, China) and U87MG cells with a 5 mL/h extrusion rate. The ratio of U87MG to MSCs in the printed coaxial fiber was 2:1. We defined the component without MSCs as Core-U87MG, and the component with MSCs as ADMSC/BMMSC + U87MG. We used 0.03 g/mL $CaCl_2$ solution and 405 nm blue-light irradiation for 3 min to cross-link them. After washing with 9 g/L NaCl solution to remove excess cross-linkers, the bioprinted microfibers were immersed in a sufficient amount of culture medium and finally moved into a cell-culture incubator with 5% $CO_2$ at 37 °C.

### Cell proliferation analysis

Cell proliferation of microfibers was analyzed with an Alamar Blue Kit (YEASEN, Shanghai, China), according to the instructions. Microfibers or 2D cells were washed with 9 g/L NaCl solution and incubated with 2 mL of working solution containing 10% Alamar Blue and 90% fresh complete medium at 37 °C for 4 h in the dark. The appropriate supernatant was transferred to a 96-well plate, and the optical density (OD) value was read at 570 and 600 nm

wavelengths (Epoch2, USA). Starting on the first day after printing, we tested the OD values of different groups in parallel every three days and finally performed a unified normalization process.

### Ca-alginate shell and GelMA core removal

The combination of 9 g/L NaCl solution with 55 mmol/L sodium citrate and 25 mmol/L ethylene diamine tetra-acetate was used to remove Ca-alginate, and GelMA lysis solution (EFL-GM-LS-001, EFL, China) was used to remove cured GelMA. After 10 min of lysis, the cells were washed and collected.

### Cell size and viability analysis

The harvested U87MG cells were mixed with the same volume of acridine orange/propidium iodide (AO/PI) solution on the smear. The smear was sent to Rigel S3 (Countstar, Shanghai, China) after mixing for a few seconds, and cell viability supplemented diameter results could then be collected on the computer.

### Immunofluorescence analysis

Immunostaining was performed to assess the expression of stem and malignant proteins of U87MG cells. Briefly, U87MG cells collected from the microfibers were directly resuspended in fresh medium to adhere to the 24-well plate, and immunofluorescence experiments were performed according to the protocol after 12 h. The cells were subsequently fixed with 4% paraformaldehyde for 20 min and blocked with blocking solution (KeyGEN, Jiangsu, China) for 30 min. Anti-Nestin, anti-CD133, anti-OCT4, and anti-GFAP (Abcam, Cambridge, UK) were diluted at recommended concentrations to incubate cells overnight at 4 °C. Secondary antibodies at a suitable concentration were added to cells for 1 h, followed by adding 4',6-diamidino-2-phenylindole (DAPI) for 5 min. Fluorescent images were taken with a fluorescence microscope (Nikon, Japan).

### Flow cytometry analysis

The harvested U87MG cells were analyzed using anti-CD105 and anti-CD133 (ThermoFisher Scientific, Waltham, MA, USA) to evaluate the expression of different phenotypes. Samples were measured on the CytoFLEX platform (Beckman Coulter, CA, USA) and analyzed with CytExpert 2.2 software.

### Western blot analysis

U87MG cells were collected from coaxial microfibers by centrifugation at 3000 r/min at 4 °C for 5 min. A total of 200 μL RIPA was added per $10^6$ cells and oscillated. After the protein was quantified with a BCA kit (KeyGEN, Jiangsu, China), 6 μg protein was separated by 10% sodium dodecyl sulfate–polyacrylamide gel electrophoresis (SDS-PAGE; Invitrogen, CA, USA) and transferred to polyvinylidene fluoride (PVDF) membranes (Millipore, CT, USA). Then, the membranes were blocked with 5% bovine serum albumin (BSA) solution for 2 h at room temperature and incubated with primary antibodies (*N*-cadherin, vimentin, Notch1, MMP2, and glyceraldehyde-3-phosphate dehydrogenase (GAPDH)) overnight at 4 °C. Membranes were stained with secondary antibody for 1 h at 37 °C, and then, the chemiluminescent substrate was uniformly added to the surface and imaged with BIOMAX-MR film (Eastman Kodak, NY, USA).

### Drug resistance analysis

To test the chemosensitivity, 2D cells and microfibers were treated with 500 μg/mL temozolomide (TMZ; Aladdin, China) solution for 48 h before replacing with fresh medium. Cell viability was examined at 48 h after treatment with Alamar Blue, as described above.

### Tumorigenesis in vivo experiment

We purchased Balb/c nude mice (3–4 weeks old, 20 g, females) from the Experimental Animal Center, Sun Yat-sen University of Medical Sciences (Guangzhou, China). The mice were randomly and equally divided into three groups: U87MG + MSC, U87MG-non-MSC, and 2D-U87MG, abbreviated as 3D87M, 3D87, and 2D87, respectively. U87MG cells were collected from each group for nude mouse tumorigenesis experiments at 7 d after bioprinting. Each nude mouse was inculcated with 0.2 mL suspension ($5 \times 10^6$ cells) and was killed by cervical dislocation after 30 d. The tumors were collected and measured with a Vernier caliper to catch the length and diameter. Tumor size was measured with a caliper, and tumor volume ($V$) was calculated according to the following formula: $V = (L \times W^2)/2$, where $L$ is length and $W$ is width.

### Statistical analysis

Each experiment was performed in triplicate, and data were presented as mean ± standard deviation (SD). Comparison between pairs of groups was evaluated using Student's *t*-tests. $P$ value of $< 0.05$ was considered statistically significant.

## Results and discussion

### Manufacturing of shell–core hydrogel microfibers and morphology of cells

The shell–core microfiber was extruded through the coaxial needle by a micro-pump (Fig. 1a). After cross-linking, the microfibers were put into six-well plates, while the shell of the microfiber was encapsulated with or without MSCs, and the core was filled with U87MG cells. In order to observe cell status, we observed the cells in the microfibers every day with a microscope (Nikon, Japan). There was not much difference among the three forms on the first day after bioprinting. Interestingly, from the fifth day, U87MG cells stretched better in the hydrogel when there were MSCs in the outer shell than when they were absent (Figs. 1b–1d). In the presence of MSCs, U87MG cells in the core stretched out like mesh, with obvious connections among them, while U87MG cells without MSCs and 2D cells preferred to arrange themselves in dots or gather together to form a cluster (Figs. 1e–1g). After 10 d of culture, U87MG cells in the MSC group filled the core and spheres in the other groups were much bigger. U87MG

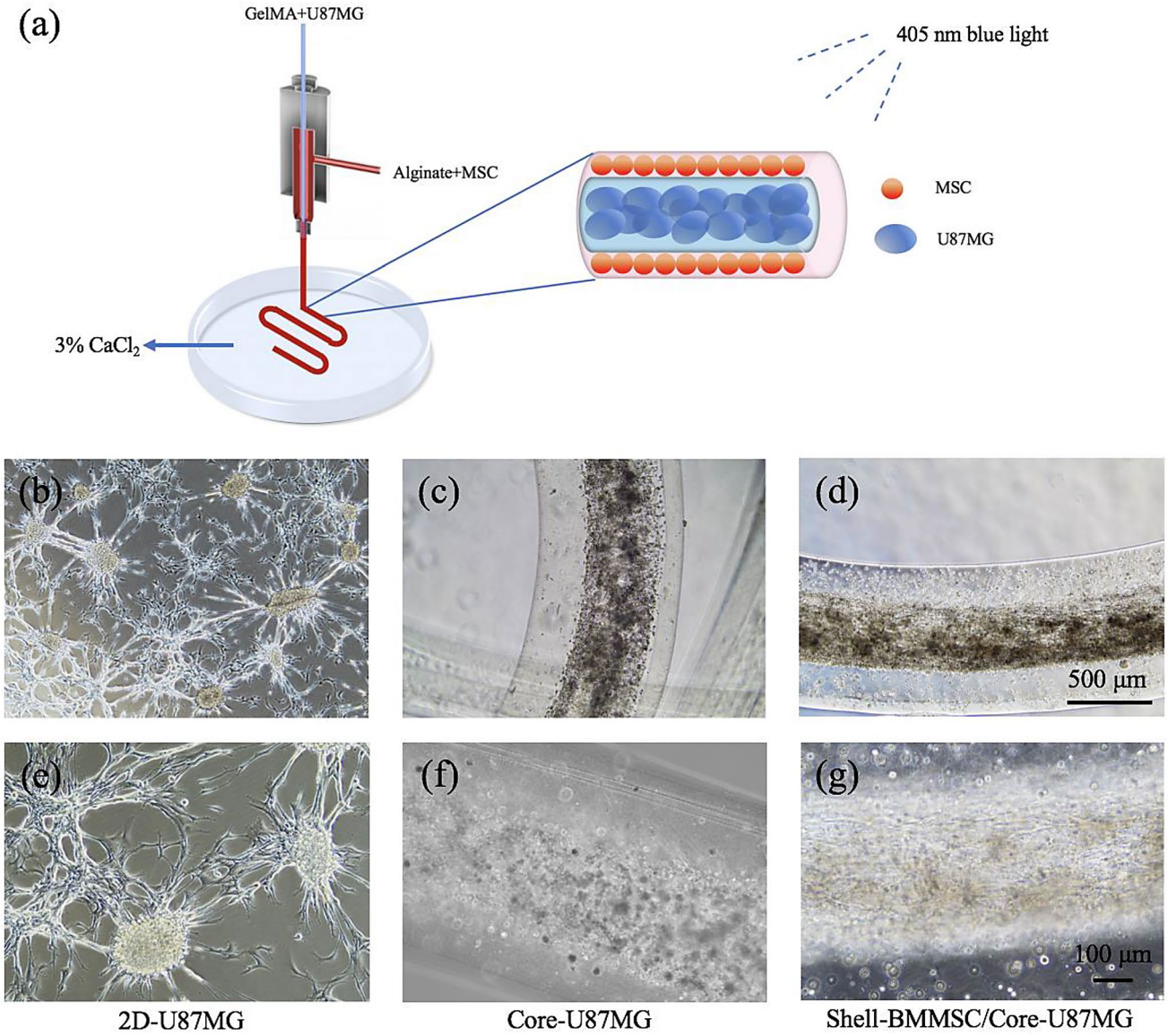


**Fig. 1** Manufacturing of coaxial Shell-MSC/Core-U87MG microfiber. **a** Schematic of the coaxial extrusion printing process, with cross-linking by $CaCl_2$ and blue light with a wavelength of 405 nm. **b–g** 2D-U87MG cells, U87MG cell fiber of Core-U87MG microfibers, and Shell-MSC/Core-U87MG microfibers were cultured for 5 d, respectively. GelMA: gelatin methacrylate; MSC: mesenchymal stem cell. Scale bars: 500 μm (**b–d**) and 100 μm (**e–g**)

cells in the MSC group continued to maintain the initial stretched state, which was very different from the other two groups. At the same time, we observed the cell size. In the presence of MSCs, the diameter of U87MG cells generally increased, which may be linked to enhancement of the migration ability of tumor cells by MSCs (Fig. 2c).

These results are quite different from those obtained with the previous printing method using alginate and gelatin, where the cells cannot be stretched and cell migration is more difficult [11]. With that method, even though the same coaxial structure is printed, the tumor cells in the hollow hydrogel are arranged in dots [12]. We speculate that there are two reasons for this phenomenon. One is that GelMA in the core provides targets for cell adhesion and migration [10], and the other is that the presence of MSCs further enhances stretching and migration ability [13].

## Cell viability and proliferation ability

In order to test whether the bioprinting process, the presence of biomaterials, or MSCs affect the survival of U87MG cells, we performed AO/PI staining 2 h and 7 d after bioprinting. We found that the survival rates of the BMMSC group ($0.8863 \pm 0.0136$) and 2D-U87MG group ($0.9010 \pm 0.0230$) were higher than that of the U87MG-non-MSC group ($0.8270 \pm 0.0227$); and the rate in the ADMSC group ($0.8410 \pm 0.0227$) was slightly higher than that of the U87MG-non-MSC group. This result shows that MSCs can also improve the survival rate of glioma cells in a 3D environment, which is consistent with the findings for 2D environments [14]. Within 2 h after printing, there was no significant difference in the survival rate of the four groups, indicating that the gentle printing and cross-linking process did not cause much damage to the cells. On the other hand, U87MG cell proliferation in the coaxial microenvironment

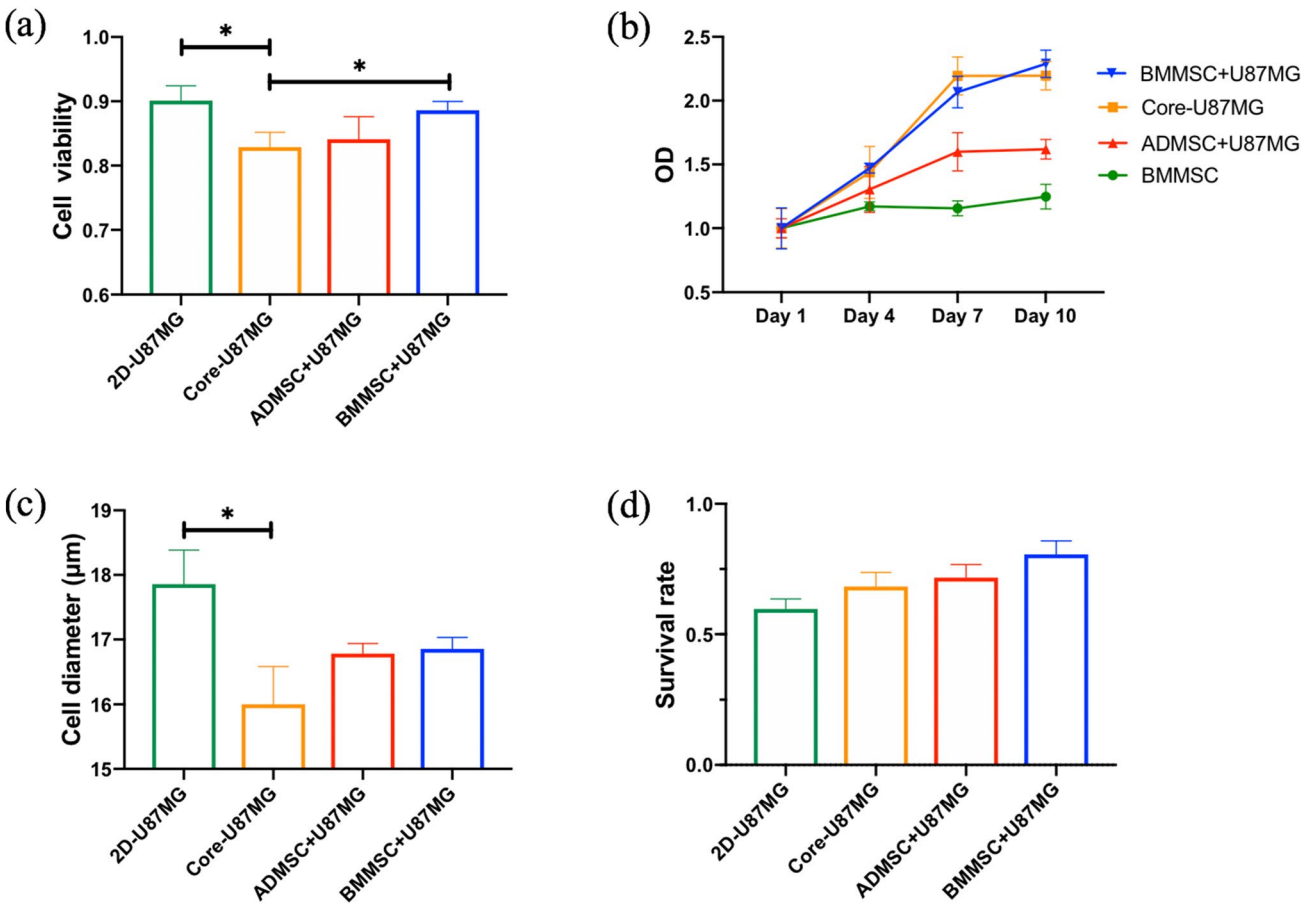


**Fig. 2** Cell viability, proliferation, diameter, and survival rate of shell–core microfibers. **a** Viability rate of cells cultured in microfibers with or without MSCs. **b** Proliferation of U87MG cells cultured in microfibers and MSCs in shell alone. **c** Cell diameter of U87MG in different microenvironments. **d** Survival rate of U87MG in TMZ at a concentration of 500 μg/mL for 48 h in various groups. Data are expressed as mean ± SD ($n = 3$). *$P < 0.05$. MSC: mesenchymal stem cell; ADMSC: adipose-derived MSC; BMMSC: bone marrow-derived MSC; OD: optical density; TMZ: temozolomide

composed of BMMSCs and ECM was much faster than that in the microenvironment without MSCs (Fig. 2b). Especially after 7 d, the non-MSC group showed signs of fatigue even in an apoptotic period, while the BMMSC group was still expanding. The MSC in shell has not proliferated much, only maintaining the role of providing nutrients [15].

## Drug resistance of Core-U87MG cells

Glioma is a highly malignant tumor, and TMZ is commonly used for chemotherapy in clinic, but the effect is usually not very satisfactory. Here, we used TMZ to observe the killing ability of this chemotherapeutic drug on glioma cells in a 3D microenvironment. When kept at a concentration of 500 μg/mL for 48 h, there were still many surviving glioma cells in the 2D group ($0.5973 \pm 0.0380$). Moreover, the Core-U87MG group ($0.6830 \pm 0.0544$), U87MG with ADMSCs group (ADMSC + U87MG, $0.7167 \pm 0.0505$), and U87MG with BMMSCs group (BMMSC + U87MG, $0.8067 \pm 0.0510$) had higher survival rates and gradually increased (Fig. 2d). These results indicate that both the ECM and MSCs in a 3D microenvironment can increase the drug resistance of glioma cells. This coaxial environment shows great potential for drug development and screening. The results may be related to the ECM that causes tumor cells to be in a hypoxic environment, which enhances tumor malignancy and the ability to resist drugs [16].

## Cell stemness, angiogenesis, and malignancy changes

Immunofluorescence results are shown in Fig. 3, which present stemness markers (CD133, Nestin, OCT4) and a malignancy marker (GFAP). In general, the microfiber which incorporated BMMSCs expressed stronger Nestin (Figs. 3d, 3h, and 3l), which may be related to the fact that tumor cells in this group were spread out, similar to the spreading state of nerve cells. Meanwhile, both coaxial groups were a little weaker in CD133 fluorescence than the 2D group (Figs. 3a, 3e, and 3i) and coaxial microfiber without MSCs was the strongest in GFAP expression (Figs. 3b, 3f, and 3j). As for the expression of OCT4, there was not much difference among the three groups (Figs. 3c, 3g, and 3k).

Stemness is an important manifestation of the malignancy of tumor cells. It enables tumor cells to renew themselves and is considered an important factor in tumor metastasis and tumor recurrence [17]. As the above results show, in a coaxial microenvironment or 3D microenvironment, BMMSCs do not increase or decrease the stemness of tumor cells, which may differ from 2D microenvironments [18].

We also used a flow cytometry method to verify the stemness changes, and the results were similar to immunofluorescence (Figs. 4a, 4b, and 4d), the only difference being that the stemness of the microfiber with ADMSCs group decreased (Fig. 4c). However, compared to the non-MSC

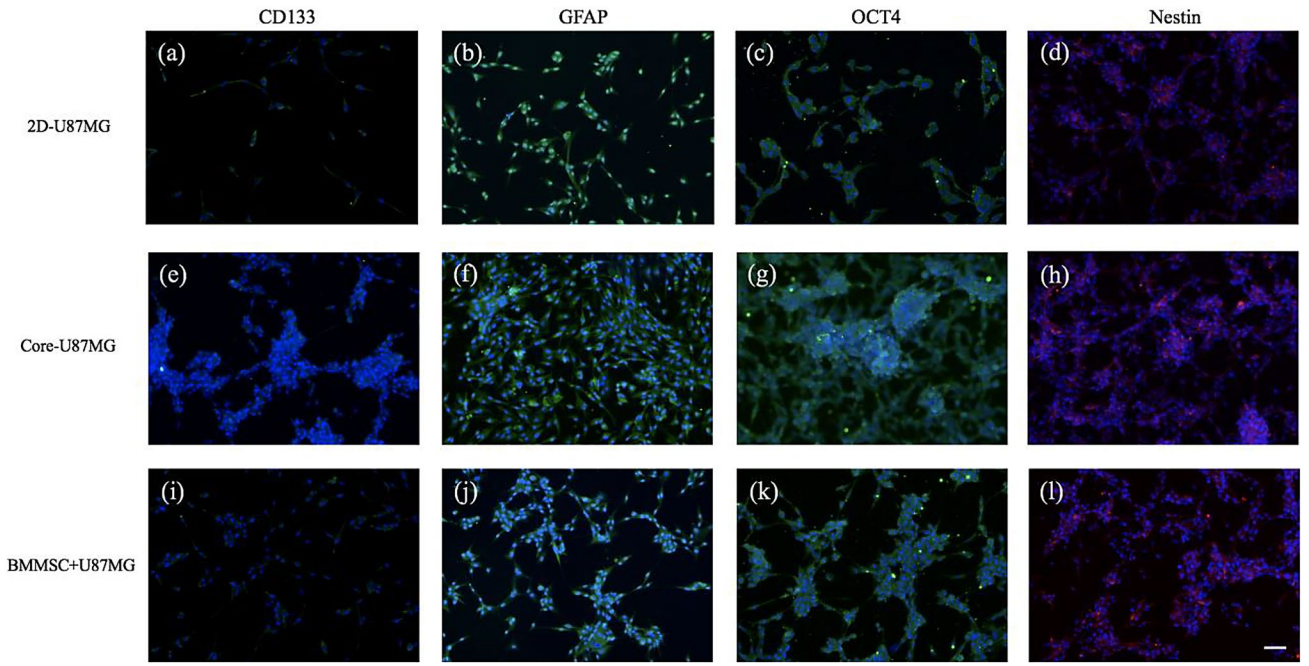


**Fig. 3** Immunostaining of CD133, Nestin, OCT4, and GFAP. **a**, **e**, **i** Merged (CD133 and DAPI) images of U87MG in different microenvironments. **b**, **f**, **j** Merged (GFAP and DAPI) images of U87MG in different microenvironments. **c**, **g**, **k** Merged (OCT4 and DAPI) images of U87MG in different microenvironments. **d**, **h**, **l** Merged (Nestin and DAPI) images of U87MG in different microenvironments. Scale bars: 100 μm. DAPI: 4',6-diamidino-2-phenylindole; BMMSC: bone marrow-derived mesenchymal stem cell

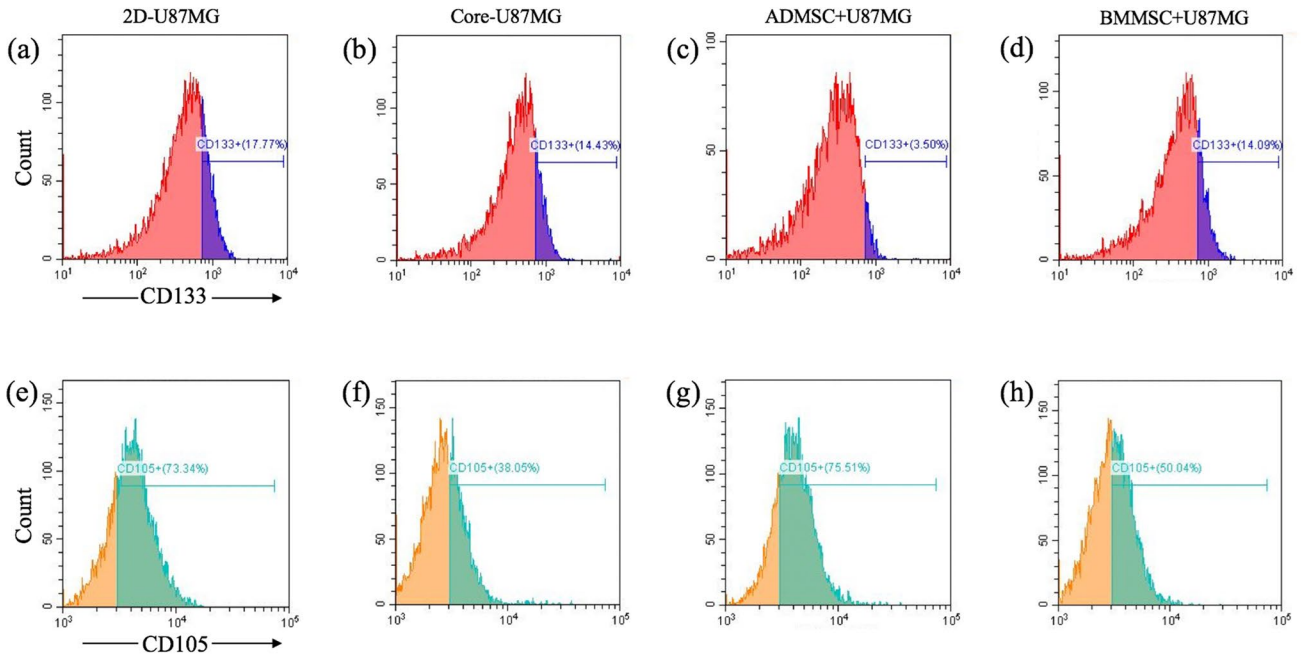


**Fig. 4** Flow cytometry of CD133 and CD105. **a**–**d** CD133 of U87MG in various groups. **e**–**h** CD105 of U87MG in various groups. BMMSC: bone marrow-derived mesenchymal stem cell. ADMSC: adipose-derived mesenchymal stem cell

group (Fig. 4f), the ADMSC and BMMSC groups expressed more CD105, a manifestation of the vascular ability of tumor cells (Figs. 4g and 4h) [19]. That means that in the presence of MSCs, tumors are likely to have more blood vessels to provide nutrition and thus will grow faster.

## Cell epithelial–mesenchymal transition and migration ability

During the development of gliomas, tumor cells secrete MMPs to digest the ECM and escape [20]. In order to determine the metastatic ability of U87MG cells in the four groups, we tested the expression ability of MMP2 in cells using Western blotting. To our surprise, coaxial fibers with ADMSC or BMMSC expressed much more MMP2 than those in the 2D and Core-U87MG groups, whose expression abilities were too low to test (Fig. 5a). This elucidates from another angle the reason for the enhanced metastasis ability of tumor cells in the presence of MSCs. Similar to this finding is the fact that the ADMSC and BMMSC groups also expressed more Notch1 protein, whose pathway promotes the proliferation of glioma cells and reduces their apoptosis (Fig. 5a) [21]. This result explains to a certain extent why U87MG proliferation becomes faster and activity becomes higher in the presence of MSCs.

EMT has recently been confirmed to play a key role in tumor occurrence, invasion, and metastasis, mainly represented by the down-regulation of E-cadherin and the up-regulation of N-cadherin and vimentin [22, 23]. We also used the above indicators to detect EMT ability in two groups; one was coaxial with low-concentration BMMSCs, and the other had high-concentration BMMSCs (Fig. 5b). When more BMMSCs existed in the shell, U87MG cells highly expressed the EMT markers N-cadherin and vimentin, which assist tumor cells to stretch out like a mesh. This makes sense because when more BMMSCs are present, U87MG cells are arranged like a mesh, and when there are fewer MSCs, the cells are arranged in clusters, but there are still intercellular connections between the clusters (Figs. 5c and 5d).

## Tumorigenic ability

To study the effect of the shell–core microfiber model on the tumorigenicity of tumor cells, we performed a tumorigenesis experiment in nude mice using the U87MG cells from the 2D (2D87), non-MSC (3D87), and MSC (3D87M) groups. Tumors visible to the naked eye were formed in the 2D87 group at 14 d. The 3D87 and 3D87M groups showed visible tumors at 20 d, and each group had one mouse that did not develop a tumor. The tumors were removed from the mice at 30 d, and various morphologies were evident. Tumorigenicity in the 3D87M and 3D87 groups was weaker than that in the 2D87 group, which may be related to a decrease in proliferation ability caused by cells being wrapped in biological material for too long and a reduction in the survival rate of tumor cells due to repeated digestion and centrifugation.

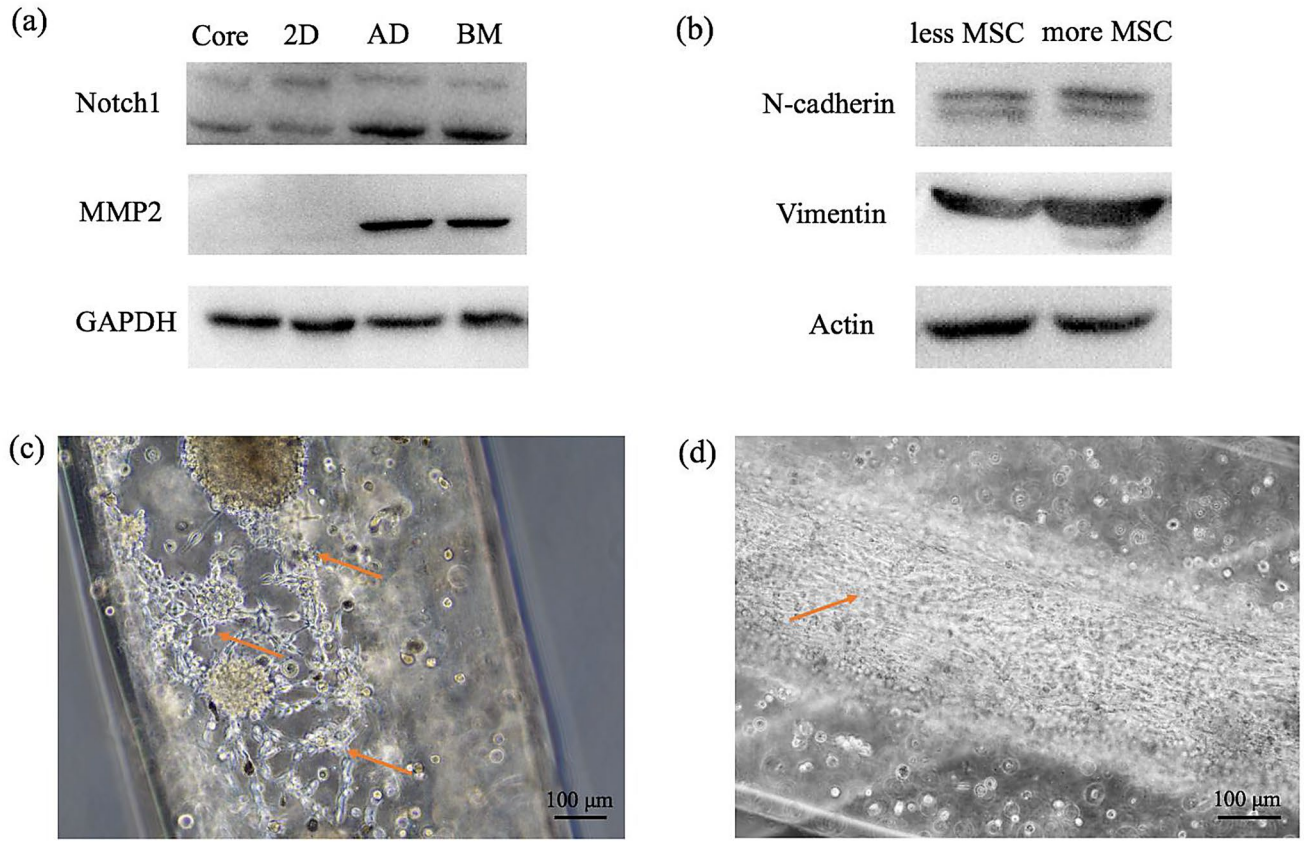


**Fig. 5** Manifestation of cell invasion and metastasis. **a** Western blot results for Notch1 and MMP2 of U87MG in various groups. Results for the ADMSC and BMMSC groups were significantly higher than those for the Core-U87MG and 2D groups. **b** EMT-related protein (N-cadherin and vimentin) expression was higher in groups with more MSCs. **c**, **d** Morphology of U87MG with fewer MSCs (**c**) and more MSCs (**d**). MSC: mesenchymal stem cell; BMMSC: bone marrow (BM)-derived MSC; ADMSC: adipose-derived (AD) MSC; MMP2: matrix metalloproteinase 2; GAPDH: glyceraldehyde-3-phosphate dehydrogenase

However, it is clear that BMMSCs enhance tumorigenicity; the 3D87M group was larger than the 3D87 group (Fig. 6).

## Conclusions

This study focused on the manufacturing of Shell-MSC/Core-U87MG hydrogel microfibers by coaxial extrusion bioprinting, in order to mimic a glioma microenvironment composed of MSCs and ECM. In this microenvironment, MSCs have the effect of promoting tumor cell spreading in the case of non-contact with U87MG. Compared with Core-U87MG hydrogel microfibers, MSCs promote U87MG cell proliferation, EMT, viability, invasion, tumorigenesis, and drug resistance and maintain stemness in Shell-MSC/Core-U87MG microfibers. What is most notable is that we found GelMA to be a suitable core biomaterial for observing tumor cell morphology, migration, and metastasis and were able to establish a coaxial coculture tumor microenvironment in vitro. This model offers a novel platform for tumor and stromal cell coculture research, to

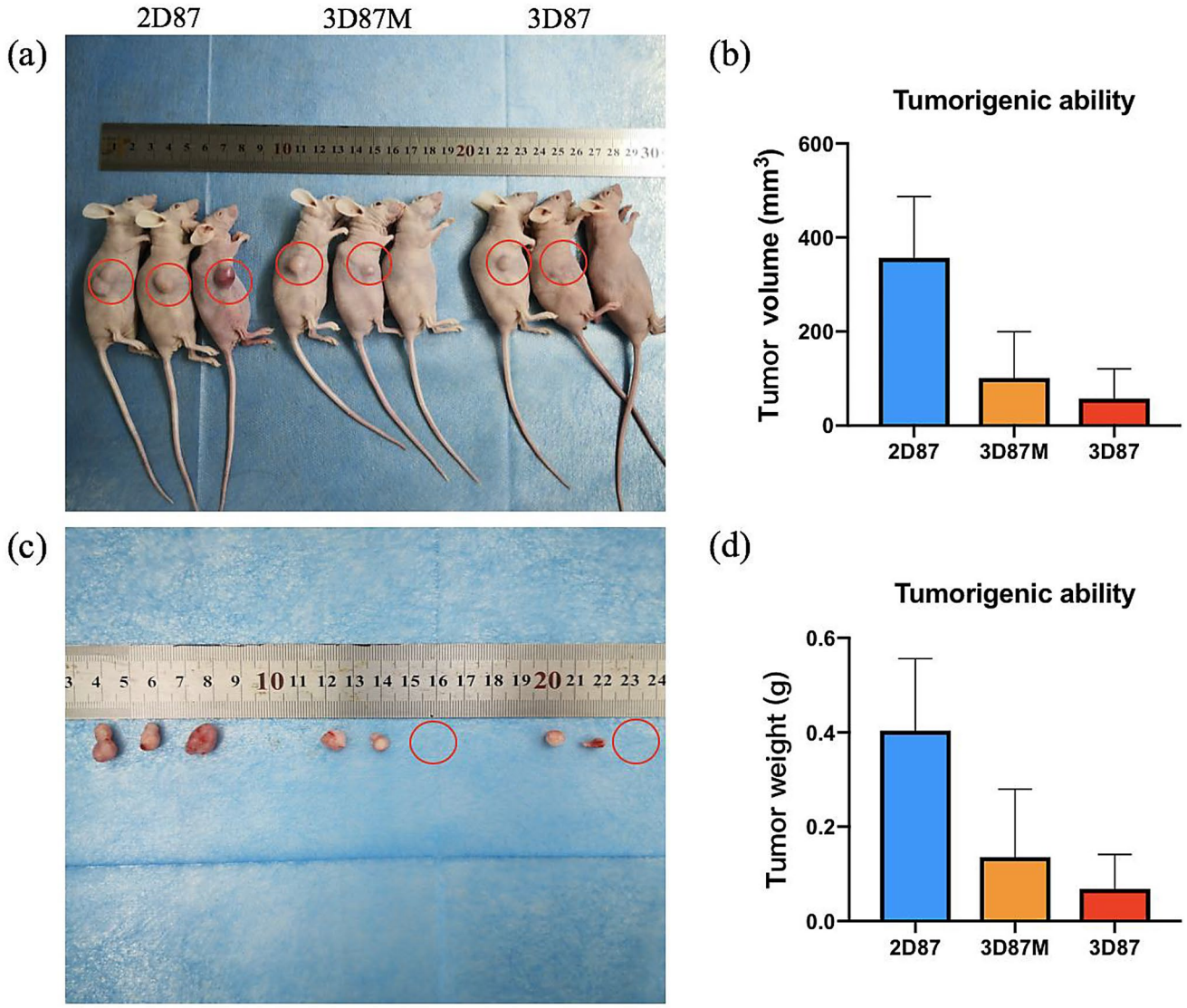


**Fig. 6** Tumor formation in animal experiment. **a** Growth condition of tumors in nude mice at 30 d post-inoculation with cells of various groups (2D-U87MG, BMMSC + U87MG, and Core-U87MG). **b** Comparison of tumor volumes among various groups. **c** Observation of tumors after removal from the body of a nude mouse at 30 d post-inoculation, with cells of various groups. **d** Comparison of tumor weight among various groups. Data are expressed as mean ± SD ($n = 3$). BMMSC: bone marrow-derived mesenchymal stem cell

reveal the mechanisms of non-neoplastic cells in ECM in vitro.

**Acknowledgements** Thanks to Jiangxi Provincial People's Government and Shangrao East China Institute of Digital Medical Engineering for their support.

**Author contributions** ZZJ participated in conceptualization, investigation, methodology, and writing of the original draft. TX and AHW contributed in conceptualization, writing, reviewing, and editing. XDL, BXL, and XRY participated in methodology and discussion. SH provided the original technique of experiments, reviewing. All authors have read and approved the final manuscript and, therefore, have full access to all the data in the study and take responsibility for the integrity and security of the data.

## Declarations

**Conflict of interest** The authors declare that there is no conflict of interest.

**Ethical approval** All animal experiments were carried out in accordance with the approved program of the Animal Care Committee of the First Affiliated Hospital of China Medical University, Shenyang, China.

## References

1. Ostrom QT, Gittleman H, Liao P et al (2014) CBTRUS statistical report: primary brain and central nervous system tumors

diagnosed in the United States in 2007–2011. Neuro Oncol 16(4):1–63. https://doi.org/10.1093/neuonc/nou223
2. Stupp R, Roila F (2009) Malignant glioma: ESMO clinical recommendations for diagnosis, treatment and follow-up. Ann Oncol 20(4):126–128. https://doi.org/10.1093/annonc/mdp151
3. Paunescu V, Bojin FM, Tatu CA et al (2011) Tumour-associated fibroblasts and mesenchymal stem cells: more similarities than differences. J Cell Mol Med 15(3):635–646
4. Ribeiro AL, Okamoto OK (2015) Combined effects of pericytes in the tumor microenvironment. Stem Cells Int 2015:868475. https://doi.org/10.1155/2015/868475
5. Nakamizo A, Marini F, Amano T et al (2005) Human bone marrow–derived mesenchymal stem cells in the treatment of gliomas. Cancer Res 65(8):3307–3318. https://doi.org/10.1158/0008-5472.CAN-04-1874
6. Nakamura K, Ito Y, Kawano Y et al (2004) Antitumor effect of genetically engineered mesenchymal stem cells in a rat glioma model. Gene Ther 11(14):1155–1164. https://doi.org/10.1038/sj.gt.3302276
7. Akimoto K, Kimura K, Nagano M et al (2013) Umbilical cord blood-derived mesenchymal stem cells inhibit, but adipose tissue-derived mesenchymal stem cells promote, glioblastoma multiforme proliferation. Stem Cells Dev 22(9):1370–1386. https://doi.org/10.1089/scd.2012.0486
8. Keramidas M, de Fraipont F, Karageorgis A et al (2013) The dual effect of mesenchymal stem cells on tumour growth and tumour angiogenesis. Stem Cell Res Ther 4:41. https://doi.org/10.1186/scrt195
9. Kucerova L, Matuskova M, Hlubinova K et al (2010) Tumor cell behavior modulation by mesenchymal stromal cells. Mol Cancer 9:129. https://doi.org/10.1186/1476-4598-9-129
10. Shao L, Gao Q, Zhao H et al (2018) Fiber-based mini tissue with morphology-controllable GelMA microfibers. Small 14(44):1802187. https://doi.org/10.1002/smll.201802187
11. Dai XL, Ma C, Lan Q et al (2016) 3D bioprinted glioma stem cells for brain tumor model and applications of drug susceptibility. Biofabrication 8(4):045005. https://doi.org/10.1088/1758-5090/8/4/045005
12. Wang XZ, Li XD, Dai XL et al (2018) Coaxial extrusion bioprinted shell-core hydrogel microfibers mimic glioma microenvironment and enhance the drug resistance of cancer cells. Coll Surf B 171:291–299
13. Ridge S, Sullivan F, Glynn S (2017) Mesenchymal stem cells: key players in cancer progression. Mol Cancer 16:31. https://doi.org/10.1186/s12943-017-0597-8
14. Iser IC, Ceschini SM, Onzi GR et al (2016) Conditioned medium from adipose-derived stem cells (ADSCs) promotes epithelial-to-mesenchymal-like transition (EMT-Like) in glioma cells in vitro. Mol Neurobiol 53(10):7184–7199. https://doi.org/10.1007/s12035-015-9585-4
15. Zhang T, Lee YW, Rui YF et al (2013) Bone marrow-derived mesenchymal stem cells promote growth and angiogenesis of breast and prostate tumors. Stem Cell Res Ther 4:70. https://doi.org/10.1186/scrt221
16. Hermida MA, Kumar JD, Schwarz D et al (2020) Three-dimensional in vitro models of cancer: bioprinting multilineage glioblastoma models. Adv Biol Regul 75:100658. https://doi.org/10.1016/j.jbior.2019.100658
17. Lathia JD, Mcak SC, Mulkearns-Hubert EE et al (2015) Cancer stem cells in glioblastoma. Genes Dev 29(12):1203–1217. https://doi.org/10.1101/gad.261982.115
18. Hossain A, Gumin J, Gao F et al (2015) Mesenchymal stem cells isolated from human gliomas increase proliferation and maintain stemness of glioma stem cells through the IL-6/gp130/STAT3 pathway. Stem Cells 33(8):2400–2415. https://doi.org/10.1002/stem.2053
19. Luo HM, Hernandez R, Hong H et al (2015) Noninvasive brain cancer imaging with a bispecific antibody fragment, generated via click chemistry. Proc Natl Acad Sci USA 112(41):12806–12811. https://doi.org/10.1073/pnas.1509667112
20. VanMeter TE, Rooprai HK, Kibble MM et al (2001) The role of matrix metalloproteinase genes in glioma invasion: co-dependent and interactive proteolysis. J Neurooncol 53(2):213–235. https://doi.org/10.1023/A:1012280925031
21. Yi L, Zhou XC, Li T et al (2019) Notch1 signaling pathway promotes invasion, self-renewal and growth of glioma initiating cells via modulating chemokine system CXCL12/CXCR4. J Exp Clin Cancer Res 38(1):339. https://doi.org/10.1186/s13046-019-1319-4
22. Martin FT, Dwyer RM, Kelly J et al (2010) Potential role of mesenchymal stem cells (MSCs) in the breast tumour microenvironment: stimulation of epithelial to mesenchymal transition (EMT). Breast Cancer Res Treat 124(2):317–326. https://doi.org/10.1007/s10549-010-0734-1
23. Xue ZF, Wu XM, Chen X et al (2015) Mesenchymal stem cells promote epithelial to mesenchymal transition and metastasis in gastric cancer though paracrine cues and close physical contact. J Cell Biochem 116(4):618–627. https://doi.org/10.1002/jcb.25013